NeuroImage 101 (2014) 380–389

Contents lists available at ScienceDirect

NeuroImage

journal homepage: www.elsevier.com/locate/ynimg

Full Length Articles

Sex differences in the relationship between white matter connectivity and creativity

Sephira G. Ryman [a,b], Martijn P. van den Heuvel [c], Ronald A. Yeo [b], Arvind Caprihan [d], Jessica Carrasco [a,b], Andrei A. Vakhtin [a,b], Ranee A. Flores [a], Christopher Wertz [a], Rex E. Jung [a,b,*]

[a] University of New Mexico Department of Neurosurgery, USA
[b] University of New Mexico Department of Psychology, USA
[c] University Medical Center Utrecht Department of Psychiatry, Netherlands
[d] Mind Research Network, USA

ARTICLE INFO

Article history:
Accepted 16 July 2014
Available online 23 July 2014

Keywords:
Creativity
Sex differences
Graph theoretical analysis
Diffusion imaging

ABSTRACT

Creative cognition emerges from a complex network of interacting brain regions. This study investigated the relationship between the structural organization of the human brain and aspects of creative cognition tapped by divergent thinking tasks. Diffusion weighted imaging (DWI) was used to obtain fiber tracts from 83 segmented cortical regions. This information was represented as a network and metrics of connectivity organization, including connectivity strength, clustering and communication efficiency were computed, and their relationship to individual levels of creativity was examined. Permutation testing identified significant sex differences in the relationship between global connectivity and creativity as measured by divergent thinking tests. Females demonstrated significant inverse relationships between global connectivity and creative cognition, whereas there were no significant relationships observed in males. Node specific analyses revealed inverse relationships across measures of connectivity, efficiency, clustering and creative cognition in widespread regions in females. Our findings suggest that females involve more regions of the brain in processing to produce novel ideas to solutions, perhaps at the expense of efficiency (greater path lengths). Males, in contrast, exhibited few, relatively weak positive relationships across these measures. Extending recent observations of sex differences in connectome structure, our findings of sexually dimorphic relationships suggest a unique topological organization of connectivity underlying the generation of novel ideas in males and females.

Published by Elsevier Inc. This is an open access article under the CC BY-NC-ND license (http://creativecommons.org/licenses/by-nc-nd/3.0/).

Introduction

Creative cognition is multifaceted, drawing on a wide range of mental faculties that enable individuals to develop novel and useful ideas (Stein, 1953). The process of creativity has been conceptualized as involving two stages: blind variation and selective retention (Campbell, 1960). The two stages utilize different brain regions in functional magnetic resonance imaging (fMRI) studies, suggesting that the blind variation and selective retention might represent distinct cognitive processes (Ellamil et al., 2012). Psychometrically, it is likely to be difficult to disentangle these two processes (Arden et al., 2010); however, divergent thinking has served as the primary measure most analogous to blind variation, as it measures an individual's ability to generate many ideas (Piffer, 2012).

Relative to the wealth of fMRI studies that have investigated divergent thinking, there are relatively few studies that have addressed the variation in underlying gray or white matter morphology and/or anatomical connectivity. Unlike other studies of cognitive abilities, increased creativity has been correlated to both increases and decreases in brain connectivity and cerebral volume elucidated through the use of proton magnetic resonance spectroscopic imaging (1H-MRSI), diffusion weighted imaging (DWI), and structural Magnetic Resonance Imaging (sMRI) (Jung et al., 2013). Two DWI investigations have examined the relationship between divergent thinking and Fractional Anisotropy (FA), a measure used to infer information about the underlying integrity of white matter fiber tracts (Johansen-Berg and Behrens, 2009). A whole brain voxel wise analysis found that increased FA near the bilateral prefrontal cortices, the body of the corpus callosum, the bilateral basal ganglia, the bilateral temporo-parietal junction and the right inferior parietal lobule was related to increased creative cognition (Takeuchi et al., 2010b). Examining FA values within a skeleton of the major white matter fiber pathways (Smith et al., 2006) Jung et al. (2010a) found lower FA to be related to increased scores on measures of divergent thinking within the left anterior thalamic radiation.

Studies that have examined volume and thickness of gray matter have found both increases and decreases across widespread regions related to higher creative cognition, with increases seen in the mid-brain,

* Corresponding author at: 801 University SE Suite 202, Albuquerque, NM 87106, USA.
E-mail address: Rex.jung@runbox.com (R.E. Jung).

http://dx.doi.org/10.1016/j.neuroimage.2014.07.027
1053-8119/Published by Elsevier Inc. This is an open access article under the CC BY-NC-ND license (http://creativecommons.org/licenses/by-nc-nd/3.0/).

striatum, precuneus, dosolateral prefrontal cortex (Takeuchi et al., 2010a), superior parietal lobule (Gansler et al., 2011), posterior cingulate and right angular gyrus (Jung et al., 2010b). Additionally, cortical decreases related to higher creative cognition were found in the lingual, cuneus, angular gyrus, inferior parietal, fusiform gyrus, orbitofrontal cortex (Jung et al., 2010b) and the splenium of the corpus callosum (Gansler et al., 2011). From these studies, it is clear that the manifestation of creativity is associated with both excitatory and inhibitory relationship between cortical and subcortical regions spanning a widespread network of brain regions (Jung et al., 2013).

From functional connectivity analysis, there is increasing evidence showing correspondence between the regions implicated in creativity and the regions identified as being within the default mode network (DMN) (Jung et al., 2013). The DMN consists of regions where neural activity is higher during the baseline state than during an experimental task (Buckner et al., 2008; Greicius et al., 2003; Raichle et al., 2001; Shulman et al., 1997), and includes the medial prefrontal cortex (MPFC), medial temporal lobes (MTLs), and the posterior cingulate cortex (PCC)/retropslenial cortex (RCS). Many cognitive functions have been attributed to the DMN, including retrieval and manipulation of past events, both personal and general, in an effort to solve problems and develop future plans (Greicius et al., 2003). Buckner and Carroll (2007) suggest that the DMN is important in remembering the past, envisioning the future and considering the thoughts and perspectives of other people, all processes that could be construed as useful to developing novel ideas within a given context (i.e., creative).

Both the functional and structural studies of divergent thinking highlight the role of widespread variations in brain-behavioral relationships associated with creative cognition, although increasing evidence suggests that the DMN and the Executive Control Network (ECN) are predominant (Jung et al., 2013). The methods used in the vast majority of studies, to date, point to individual regions implicated in creativity; relatively few examined creativity in context of the network structure of the human brain. Instead of investigating the role of specific regions and pathways in isolation, fiber tractography can be used to construct and examine all of the connections in the brain, known as a connectome (Bullmore and Sporns, 2009; Craddock et al., 2013). By representing this information as a graph, measures of network organization can be extracted that indicate the extent of segregation and integration of connections (Rubinov and Sporns, 2010). Initial studies utilizing this approach characterized the brain as having a "small world" organization: in other words, the brain is organized such that there is a balance between local, clustered connectivity and global, long-range connectivity that facilitates efficient information transfer (Achard et al., 2006; Eguiluz et al., 2005; Sporns et al., 2004; Stam and Reijneveld, 2007b; van den Heuvel et al., 2008). The small world organization facilitates efficient information transfer via local processing within clusters that work in conjunction with several long-distance connections (Bullmore and Sporns, 2009; Latora and Marchiori, 2001; Watts and Strogatz, 1998a).

Small worldness is determined through the quantification of minimum path length, the shortest path needed to move from node *i* to *j* in a network, and clustering coefficient, the extent to which a node's neighbors are connected to each other (Bassett and Bullmore, 2006; Humphries and Gurney, 2008; Watts and Strogatz, 1998b). Using similar information, Latora and Marchiori (2001) proposed a measure of Global Efficiency that directly quantifies how efficiently information can be exchanged over the network. Evidence emerging through the use of both structural (diffusion weighted imaging) and functional imaging (fMRI, MEG) demonstrates that these measures are, in a general sense, quantifying local processing (high clustering) with an optimum number of long range paths (high efficiency) (Bullmore and Sporns, 2009; Stam and Reijneveld, 2007a). There is also growing interest in how these structural networks relate to the functional networks, with studies finding that the functional connectivity network organization is constrained by the underlying structural organization. In other words, the functional network can only be as efficient and clustered as its underlying connectivity (Greicius et al., 2009; Honey et al., 2009; van den Heuvel and Sporns, 2013a,b; van den Heuvel et al., 2009).

Individual differences in these network properties (i.e., higher efficiency) have been linked to measures of individual differences including intelligence (Li et al., 2009; van den Heuvel et al., 2009), and are being increasingly used to identify how variations in network metrics relate to cognitive dysfunction (de Haan et al., 2012; Fair et al., 2010). Several studies have found substantial sex differences in brain connectivity, suggesting that differential connectivity patterns may account for cognitive differences (Gong et al., 2009a, 2011; Ingalhalikar et al., 2013). While these studies posit potential cognitive differences resulting from the differing organization of male and female brains, they did not examine this relationship directly. Using other brain measures, such as the grey matter and white matter volumes and the functional and structural connectivities, there are numerous studies identifying sex differences in the relationship between brain measures and cognitive abilities (Gur et al., 1999), particularly with respect to higher order cognition, such as intelligence (Haier et al., 2005; Jung et al., 2005; Schmithorst, 2009; Schmithorst and Holland, 2007). In light of the recent studies emphasizing sex differences in structural brain organization and previous sex interactions in the relationship between brain structure and cognitive ability, this study investigates whether structural network properties significantly relate to creativity and whether the relationship between the structural connectome and creativity differ by sex. Second, we investigate whether variations in the network properties of individual regions of the brain are predictive of divergent thinking and if these regions are primarily within the DMN and ECN.

Materials and methods

Participants

Participants were young adults (21.53 +/− 2.93 years; 59 males, 47 females) recruited by postings in various departments and classrooms around the University of New Mexico. This study was conducted according to the principles expressed in the Declaration of Helsinki, and was approved by the Institutional Review Board of the University of New Mexico. All subjects provided written informed consent before the collection of data and subsequent analysis. One hundred and nineteen volunteers, with no history of neurological or psychological disorder, participated in the study. Thirteen individuals were excluded in the data analysis due to the low quality of their neuroimaging data (i.e. motion or image artifacts), resulting in 106 human subjects for analysis.

Behavioral measures

Four divergent thinking tasks were administered: Verbal and Drawing Creativity Tasks, Uses of Objects Test (UOT), described in detail elsewhere (Lezak et al., 2004; Miller and Tal, 2007) and generation of captions to New Yorker Magazine cartoons. Four independent judges (two females, two males) ranked the DT products of each participant using the consensual assessment technique (Amabile, 1982) from which a "Composite Creativity Index" (CCI) was derived. The raters were of the same cohort as the subjects (19–29; college student/graduate). Raters were instructed to rate each subject's DT product from 1 (lowest creativity) to 5 (highest creativity) according to their own notion of "creativity," and were instructed to bin rankings to conform to a normal distribution (e.g., 5% each 1's and 5's, 10% each 2's and 4's, 70% 3's). Rankings for each subject were averaged across the four measures and converted to a standard score to facilitate easy comparisons between FSIQ and the creativity measure, referred to as the Composite Creativity Index (CCI). The raters had excellent inter-rater reliabilities across the four measures of DT (i.e., CCI $\alpha = .81$).

To assess general intelligences, subjects were tested with the Wechsler Adult Inventory Scale (WAIS-III) (Wechsler, 1981). The

WAIS battery consists of subtests that measure verbal and non-verbal mental abilities that contribute to general intelligence. The Full Scale Intelligence Quotient (FSIQ) was based on performance on 11 subtests (Comprehension, Picture Arrangement, Object Assembly were not administered).

Imaging acquisition

Imaging was obtained using a 3 Tesla Siemens Triotim MRI using a 12-channel head coil. The multiecho MPRAGE protocol was followed to obtain the T1 image: [TE 1.64/3.5/5.36/7.22/9.08 ms; TR 2530 ms; voxel size 1 × 1 × 1 mm; 192 slices; Field of View = 256 mm; acquisition time 6.03]. For the diffusion weighted imaging (DWI) data echo planar imaging was acquired: [TE 84 ms; TR 9000 ms; voxel size 2 × 2 × 2 mm^3; 72 slices; Field of View = 256 mm; 2 set of 30 diffusion directions with b = 800 s/mm^2, and 5 measurements with b = 0, acquisition time 5:42].

DWI preprocessing and deterministic fiber tracking

The two sets of 30 diffusion directions and 5 b = 0 were concatenated to increase the signal to noise ratio (60 directions, 10 b = 0 total). The remaining processing of the DWI images followed the methods previously described in detail (van den Heuvel and Sporns, 2011). First, diffusion weighted images were realigned and registered to the first b = 0 image, and corrected for eddy-current distortions. Second, a tensor was fitted to the diffusion profile within each voxel using a robust tensor fitting method (Chang et al., 2005). The preferred diffusion direction within each voxel was computed as the principal eigenvector of the eigenvalue decomposition of the fitted tensor. Third, the level of fractional anisotropy (FA) of each voxel was computed based on the eigenvalues. Fourth, the white matter tracts of the brain networks were reconstructed by using the deterministic fiber tracking, based on the FACT (fiber assignment by continuous tracking) algorithm utilizing an FA threshold of 0.1 and an angular threshold of 45° (Mori and van Zijl, 2002).

T1 preprocessing

The MPRAGE T1 images were used for anatomical references and for the selection of the nodes of the brain network. Freesurfer was used to classify the grey matter and white matter of the brain as well as automatically segment the subcortical structures (i.e. the brain stem, thalamus, pallidum, caudate, putamen, accumbens, hippocampus, and amygdala). Automatic parcellation of the reconstructed cortical surface segmented the images into 68 distinct brain regions (V5; http://surfer.nmr.mgh.harvard.edu/ Fig. 1a) (Fischl et al., 2004). In total, eighty-three brain regions were selected, representing the nodes of the individual brain networks.

FA- and NOS- weighted reconstruction of individual structural networks

Individual brain networks were modeled based on segmented brain regions and the collection of reconstructed fiber tracts (Hagmann et al., 2008; van den Heuvel et al., 2010). The network was mathematically described as a graph G = (V,E), with V being the collection of 83 regions and E the set of the reconstructed white matter pathways between

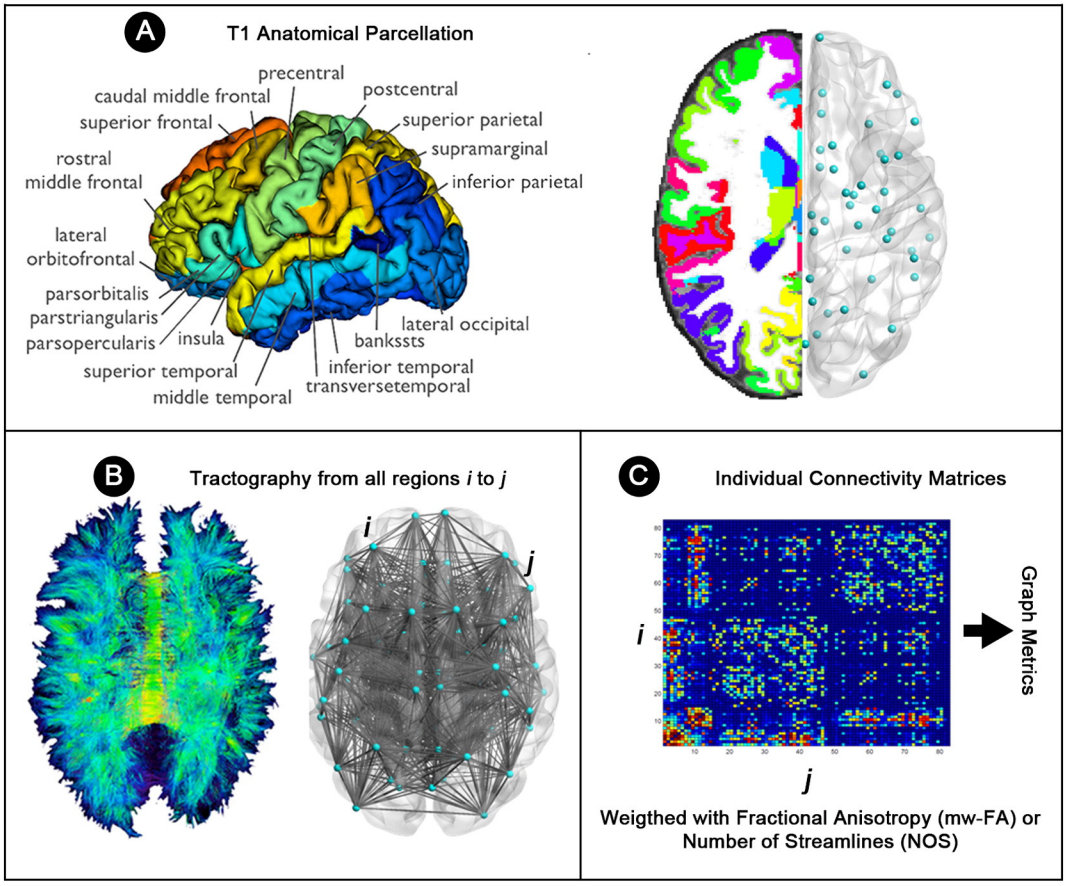

Fig. 1. Structural network reconstruction. A, First, the T1 images were segmented using freesurfer B, the DWI data was processed and all of the possible fibers in the brain were computed using deterministic fiber tracking. The number of streamlines as well as the overall integrity of the connections was calculated for each of the freesurfer regions represented here as nodes. C, for each combination of regions i and j nodes of the network, the presence of a connection was determined by those tracts that touched both region *i* and region *j*, and the average integrity of each of the tracts (as measured by FA) was entered into the matrix (w_{ij}). From the resulting individual weighted matrices, graph metrics, such as clustering coefficient and efficiency were computed.

these regions. For each subject, the presence of a reconstructed fiber streamline between each pair of brain regions *i* and *j* was taken to determine the presence of a connection between region *i* and *j* (Fig. 1b). To obtain information not only about the presence of a connection, but also about the strength and integrity of the connection, a metric utilizing information about the mean of the FA value was created (w), the average FA values of all included streamlines. This value was then entered in the FA-weighted connectivity matrices (G) as w_{ij} (Fig. 1c). An additional edge weighting, number of streamlines (NOS), was used to determine the robustness of our findings. For the NOS-weighted connectivity matrices (G), w_{ij} is equal to the number of tractography streamlines found to connect regions *i* and *j*.

Graph metrics

Graph metrics were computed using the Brain Connectivity Toolbox as described previously (Rubinov and Sporns, 2010). Graph metrics were calculated separately for each of the weighted connectivity matrices (FA-weighted and NOS-weighted). Weighted connectivity strength of each node *i* (S_i) in the network provides information about the total level of the weighted connectivity of a node. By taking this approach, the S weighted measure reflects both the number of connections in the whole brain and the fidelity of those connections quantified by either the average FA across the tracts or the NOS (Eq. (1)):

$$S_i^{weighted} = \sum_{j\in N} w_{ij}. \tag{1}$$

The total connection strength of the network (S) was calculated as the sum of S_i in all nodes N (Eq. (2)). For the FA weighted matrices, this value is the sum of the average FA values for each connection from region *i* to *j*. For the NOS weighted matrices, this value corresponds to the total sum of the number of streamlines connecting regions *i* to *j*.

$$S^{weighted} = \frac{1}{N}\sum_{i\in N} S_i. \tag{2}$$

Weighted clustering coefficient of the network (C) and of each node (C_i) is used to quantify the extent of segregation in the brain, allowing for specialized processing to occur within densely interconnected groups of brain regions (Rubinov and Sporns, 2010; Watts and Strogatz, 1998b). C_i for each node *i* corresponds to the number of the connections between all the neighbor nodes of region *i*, including information on how strong node *i* and its direct neighbors are clustered (Eq. (3)).

$$C_i^{weighted} = \frac{\sum_{j,h\in N}\left(w_{ij}w_{ih}w_{jh}\right)^{\frac{1}{3}}}{k_i(k_i-1)} \tag{3}$$

With weighted node degree of *i* (Eq. (4))

$$k_i^w = \sum_{j\in N} w_{ij}. \tag{4}$$

Nodes with only one connection were assigned a C_i of 0. The overall clustering-coefficient C characterizes the overall clustering of G and was computed as the average of C_i over all voxels *i* in G (Eq. (5)).

$$C^{weighted} = \frac{1}{N}\sum_{i\in N} C_i^{weighted}. \tag{5}$$

Weighted local and global efficiencies provide information about the integration of information from distributed brain regions. Paths in a network are sequences of distinct links between nodes that represent route of information flow (Latora and Marchiori, 2001). In weighted graphs, the distance matrix ($d^{weighted}$) is the inverse of the connection strength, w (Eq. (6)). Weighted efficiency (Effi) is calculated as the average inverse shortest path length from region *i* to all other regions *j* in the network (Eq. (7)).

$$E_i^{weighted} = \frac{1}{2}\sum_{i\in N}\frac{\sum_{j,h\in N, i\neq}\left(w_{ij}w_{ih}\left[d_{jh}^{weighted}(N_i)\right]^{-1}\right)^{1/3}}{k_i(k_i-1)}, \tag{6}$$

with

$$d^{weighted}(i,j) = \sum_{u,v\in g^w}\frac{1}{w_{uv}}. \tag{7}$$

Global efficiency is similarly calculated as the average inverse shortest path length across the whole network (Eq. (8)).

$$E^{weighted} = \frac{1}{n}\sum_{i\in N}\frac{\sum_{j\in N, j\neq i}\left(d_{ij}^w\right)^{-1}}{n-1}. \tag{8}$$

Statistics

Global metrics

As the distribution properties of most graph metrics are poorly characterized, nonparametric statistical tests were used to examine the relationship between graph metrics and CCI as well as the sex interaction (Bullmore and Sporns, 2009; Craddock et al., 2013). To examine the relationship between CCI and global graph metrics calculated from FA weighted connectivity matrices, permutation testing was used. First, the observed correlation between the global statistic (S, C, and E separately) and CCI was calculated for the whole group (r_{obs}). The data was then permuted, randomly reassigning group (male or female) for 10,000 permutations (B). For each B, the observed correlation between the global statistic and CCI was calculated. The p-value was calculated as the probability of obtaining correlations that are more extreme than the observed correlations. To remove the effects of FSIQ, the analysis was conducted again following the same procedure, however, the correlations between CCI and the graph metric of interest were conducted after the effects of FSIQ were regressed out of the CCI measure. The C and E measures are dependent on the underlying structural connectivity (S). To ensure the effects of C and E are due to the organization of the connectivity, the effect of connectivity (S) was also regressed out of the CCI measure. By taking this approach, we know that the relationships are due to the organizational properties rather than the underlying connectivity.

For results with a significant correlation between the CCI and the graph metric, tests of the interaction of sex were conducted to determine if the correlations between CCI and graph metric differed at the level of sex. First, the observed correlation between global statistic (S, C, and E separately) and CCI was calculated within each sex ($r_{obsFemale}$ $r_{obsMale}$). Second, the absolute value of the difference between the correlations was computed. Third, the permutation step consisted of the random reassignment of group (male or female). This was conducted for 10,000 permutations (B). For each B, the absolute values of the differences in correlations between the global statistic and CCI were computed, with each permuted correlation coefficient r^*_{Female} and r^*_{Male}. From this, we obtained a distribution of the differences in correlation coefficients. The p-value was calculated as the probability of obtaining differences in correlations that are more extreme than the observed difference in correlations. To remove the effects of age and FSIQ, the analysis was conducted again following the same procedure, however, the correlations between CCI and the graph metric of interest were conducted after the effects of age and FSIQ were regressed out of the CCI measure. For the analyses of clustering and efficiency, the effect of connectivity (S) was also regressed out of the CCI measure to ensure that any significant relationships found are not driven by the total connectivity, but by the topological organization of connectivity.

If significant differences in correlations were found between the sexes, each global graph metrics was then examined within each sex. Permutation procedures were followed as above, however, examining only the correlation to determine the probability of obtaining correlations as extreme or more extreme that the observed correlation within each sex separately.

The same procedure outlined above was followed to analyze the NOS-weighted connectivity matrices.

Region specific metrics

Region specific metric analyses were run if the global interaction was significant. To examine the relationship between CCI and region specific graph metrics calculated from the weighted connectivity matrices, permutation tests were used. The first analyses examined the difference in correlations between regional graph metric and creativity between males and females. The same permutation procedure was conducted as with the global metrics, examining the observed absolute value of the difference in correlations between node statistic (S_i, C_i, and E_i) and CCI. For each node i, 10,000 permutations were conducted. To identify which regions within each sex were related to creativity, an additional analysis examined the strength of the correlations in males and females separately. First, the correlation coefficients were calculated within each sex ($r_{obsFemale}$ $r_{obsMale}$). Second, the group assignments (male or female) were then randomly reassigned and the correlation between the node statistic and CCI was computed. This was conducted for 10,000 permutations (B), with each permuted correlation coefficient, r^*_{Female} and r^*_{Male}. The p-value was calculated as the probability of obtaining correlations through permutations that are more extreme than the observed correlations. To correct for multiple comparisons, effects were tested to determine if they survived a False Discovery Rate (FDR) threshold of $q = 0.05$ (Benjamini and Hochberg, 1995) across all node specific measures.

Results

There were no significant differences in age and CCI in males and females (Table 1). Similarly, no significant differences in the global (Table 1) and local graph metrics were observed, corrected for multiple comparisons. There were, however, significant differences in FSIQ, with males scoring (on average) significantly higher than females (Table 1).

Global metrics

The first analyses between global metrics (S, C, and E) calculated from the FA-weighted connectivity matrices revealed a significant correlation between clustering (C) and creativity in the entire group, accounting for age, sex, and total connectivity strength (S). The relationship between global connectivity (S) and CCI differed across the sexes ($p = 0.006$, $p < 0.001$ when accounting for age and FSIQ). For clustering (C), there were significant differences in the correlations between the global metrics and creativity in each sex when accounting for age, connectivity (S), and FSIQ ($p = 0.02$; Fig. 2). There were no significant differences in the correlations between CCI and efficiency (E) in each sex accounting for age, connectivity (S), and FSIQ. When the relationship between CCI and S was examined in each sex separately, there was a significant negative correlation between S and CCI when accounting for age and FSIQ ($p = 0.025$). There was no significant relationship between S and CCI in males. When the relationship between CCI and C was examined in each sex separately, there was a significant negative correlation between C and CCI when accounting for age, FSIQ, and connectivity (S; $r = -0.51$, $p < 0.001$; Fig. 2). There was no significant relationship between S and CCI in males (Fig. 2).

The NOS weighted matrices revealed no significant results, suggesting that the observed FA effects are likely not related to simple difference in tractography across subjects.

Table 1
Group differences.

Cognitive variables and graph metrics	Males, mean ± SD	Females, mean ± SD	p-Value
CCI	98.27 ± 8.92	99.76 ± 9.37	0.4137
FSIQ	121.08 ± 14.04	115.25 ± 12.15	0.0265*
Age	21.62 ± 2.80	21.40 ± 3.09	0.6932
Connectivity $S^{weighted}$	620.01 ± 65.87	604.04 ± 69.67	0.4633
Clustering $C^{weighted}$	0.540 ± 0.01	0.536 ± 0.01	0.1741
Efficiency $E^{weighted}$	0.941 ± 0.01	0.943 ± 0.01	0.2374

FSIQ, Full-Scale Intelligence Quotient; CCI, Composite Creativity Index; connectivity $S^{weighted}$, clustering $C^{weighted}$, efficiency $E^{weighted}$.
* Indicates significance at $p < 0.05$.

Region specific metrics

Significant differences in correlations at each level of sex

The correlations between S and C for each region i and creativity significantly differed in males and females in regions primarily within the frontal and parietal lobes, but also within the occipital, temporal, and subcortical regions (Table 2). For each of the regions that demonstrated significant differences in correlations, females demonstrated negative correlations between each graph metric and CCI, while males demonstrated either positive correlations or correlations close to zero (Fig. 3). When the effects of FSIQ were not accounted for, results did not significantly differ. Similarly, when S was accounted for in the analyses of C and E, the results did not significantly differ, indicating that the effects were not driven by total connectivity but by the topological organization.

Significant relationships between node specific connectivity S_i and creativity

The results of the permutation testing revealed that females exhibited significant negative correlations between connectivity S_i in regions of the frontal and parietal lobes, as well as a subcortical regions accounting for age and FSIQ. Males exhibited significant positive correlations between connectivity S_i in accounting for age and FSIQ (Fig. 4). Specifically, in females the left banks of the temporal lobe ($p = 0.0012$*, * indicates region survived critical FDR threshold for multiple comparisons), left caudal anterior cingulate ($p = 0.0218$), right caudal anterior cingulate ($p = 0.0050$*), right entorhinal ($p = 0.0180$), right fusiform ($p = 0.0043$*), right inferior parietal ($p = 0.0023$*), right lateral occipital ($p = 0.0285$), right parahippocampal ($p = 0.0049$*), right posterior cingulate ($p = 0.0054$), right rostral middle frontal ($p = 0.0482$), right superior frontal ($p = 0.0054$), and right accumbens area ($p = 0.0012$*) demonstrated significant negative correlations between S_i and CCI, accounting for age and FSIQ. In males, the left middle temporal ($p = 0.018$), right rostal middle frontal ($p = 0.0438$), and right amygdala ($p = 0.0226$) demonstrated significant positive correlations between S_i and CCI, accounting for age and FSIQ.

Significant relationships between node specific connectivity E_i and creativity

The results of the permutation testing revealed that females exhibited significant negative correlations between connectivity E_i in regions of the frontal and parietal lobes, as well as subcortical regions, corrected for age and FSIQ. Males exhibited significant positive correlations between connectivity E_i, accounting for age and FSIQ (Fig. 4). Specifically, in females the left banks of the temporal lobe ($p = 0.0288$), left caudal anterior cingulate ($p = 0.0135$), left medial orbitofrontal ($p = 0.0327$), left rostral anterior cingulate ($p = 0.0187$), left rostral middle frontal ($p = 0.0102$), left temporal pole ($p = 0.027$), right amygdala ($p = 0.0262$), right caudal anterior cingulate ($p = 0.0074$), right entorhinal ($p = 0.0167$), right fusiform ($p = 0.0272$), right inferior parietal ($p = 0.0046$), right inferior temporal ($p = 0.0391$), right isthmus of the cingulate ($p = 0.0298$), right lateral orbitofrontal ($p = 0.0154$),

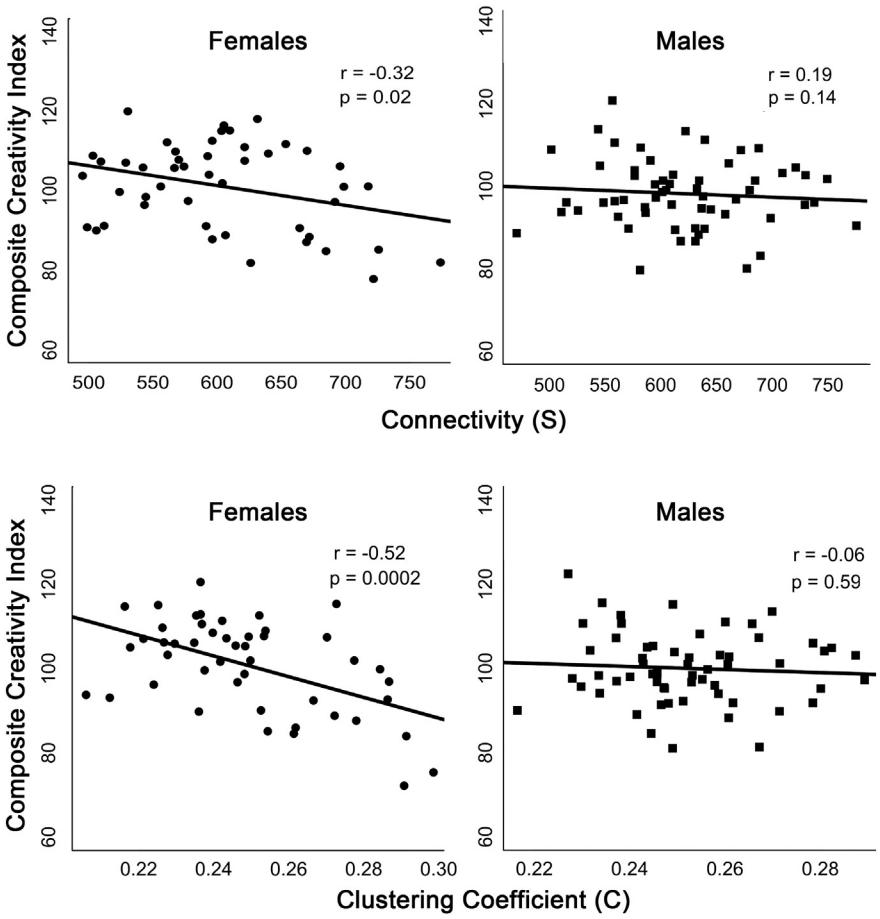

Fig. 2. Scatter plots depicting the relationship between the global measure of network Connectivity (S), the global measure of clustering observed in the metric (C) and Creativity in each sex separately. Females exhibit significant negative correlations between graph metrics and creativity, whereas male show no significant relationships.

right posterior cingulate ($p = 0.0022$), right superior frontal ($p = 0.0061$), right temporal pole ($p = 0.0018^*$), right caudate ($p = 0.0116$), right amygdala ($p = 0.0262$), and right accumbens area ($p = 0.0004^*$) demonstrated significant inverse correlations between E_i and CCI accounting for age and FSIQ. Whereas males demonstrated significant positive correlations between the left inferior parietal ($p = 0.0214$), left middle temporal ($p = 0.0199$), and right rostral middle frontal ($p = 0.0305$) and CCI accounting for age and FSIQ.

Significant relationships between node specific connectivity C_i and creativity

The results of the permutation testing revealed that females exhibited significant negative correlations between connectivity C_i in regions of the frontal and parietal lobes, as well as subcortical regions, accounting for age and FSIQ. Males exhibited significant positive correlations between connectivity C_i, accounting for age and FSIQ (Fig. 4). Specifically, the left banks of the temporal lobe ($p = 0.0288$), left caudal anterior cingulate ($p = 0.0135$), left medial orbitofrontal ($p = 0.0327$), left rostral anterior cingulate ($p = 0.0187$), left rostral middle frontal ($p = 0.0102$), left temporal pole ($p = 0.0270$), right caudal anterior cingulate ($p = 0.0074$), right entorhinal ($p = 0.0167$), right fusiform ($p = 0.0272$), right inferior parietal ($p = 0.0046$), right inferior temporal ($p = 0.0391$), right isthmus cingulate ($p = 0.0391$), right lateral occipital ($p = 0.0298$), right lateral orbitofrontal ($p = 0.0154$), right posterior cingulate ($p = 0.0022$), right superior frontal ($p = 0.0061$), right temporal pole ($p = 0.0018$), right caudate ($p = 0.0116$), right amygdala ($p = 0.0262$), and right accumbens area ($p = 0.0004^*$).

Discussion

This study of large-scale brain connectivity reveals that the relationships between connectivity of the brain and creativity differ in females and males, accounting for age and intelligence. Extending previous observations of connectome differences between males and females (Ingalhalikar et al., 2013) our findings now show a sexually dimorphic relationship of connectome structure on creativity. Males showed positive, but weak relationships between graph metrics and creativity, while females were found to exhibit an inverse relationship between connectivity and clustering of the global structural network and creativity.

Region specific analyses provided further insight into these differences, with more creative females demonstrating lower connectivity, efficiency, and clustering in numerous regions across the brain and more creative males exhibiting greater connectivity, efficiency, and clustering in relatively fewer regions. These differing relationships suggest that, at the expense of efficiency (greater path lengths), highly creative females are able to develop novel ideas to solutions by involving more regions of the brain in processing. Highly creative males, in contrast, demonstrate more efficiency and clustering of the network, suggesting more direct connections between regions as well as an increase in local processing. The regions implicated include regions of the DMN and the ECN, suggesting that these networks are critically involved in creativity as measured by divergent thinking. We note that these results are consistent with the emerging data that supports the involvement and interaction of the DMN and the ECN in creative thinking, as reviewed elsewhere (Jung et al., 2013). Furthermore, we found significant relationships between creativity and regions such as the thalamus,

Table 2
Group differences in correlations.

Regions that significantly differ in the correlations between graph metric and CCI		Connectivity		Efficiency		Clustering	
		$r_{obsFemale}-r_{obsMale}$	p-Value	$r_{obsFemale}-r_{obsMale}$	p-Value	$r_{obsFemale}-r_{obsMale}$	p-Value
Subcortical	Left_caudate	−0.3494	0.0169	−0.4627	0.0011[a]		
	Left_accumbens_area			−0.4196	0.0039[a]	−0.3246	0.0256
	Right_putamen					−0.4257	0.0031[a]
	Right_thalamus_proper	−0.3091	0.0347	−0.3102	0.0377		
	Right_caudate	−0.3722	0.0112	−0.4446	0.0017[a]		
	Right_hippocampus			−0.3546	0.0143[a]	−0.3263	0.0269
	Right_amygdala	−0.5384	0.0001[a]	−0.5718	0.0001[a]	−0.3198	0.0306
	Right_accumbens_area	−0.5686	0.0002[a]	−0.6496	0.0001[a]		
Default mode network	Left caudal anterior cingulate	−0.5111	0.0002[a]	−0.4743	0.0011[a]		
	Left cuneus			−0.3386	0.0209	−0.3546	0.0150[a]
	Left fusiform					−0.5750	0.0001[a]
	Left inferiorparietal	−0.3034	0.0381	−0.4567	0.0009[a]	−0.4001	0.0053[a]
	Left isthmus cingulate			−0.3009	0.0398		
	Left entorhinal	−0.3594	0.0145			−0.4135	0.0044[a]
	Left posterior cingulate					−0.5360	0.0001[a]
	Left precuneus					−0.3038	0.0360
	Left rostral anterior cingulate	−0.3942	0.0072	−0.5421	0.0001[a]	−0.4339	0.0029[a]
	Right cuneus					−0.3212	0.0300
	Right caudal anterior cingulate	−0.3308	0.0248	−0.3586	0.0157[a]		
	Right entorhinal	−0.4961	0.0005[a]	−0.5121	0.0003[a]	−0.3536	0.0139[a]
	Right fusiform	−0.4967	0.0004[a]	−0.4754	0.0008[a]	−0.5095	0.0005[a]
	Right inferiorparietal	−0.4993	0.0004[a]	−0.5534	0.0002[a]	−0.2928	0.0435
	Right parahippocampal	−0.2964	0.0438			−0.3528	0.0147[a]
	Right posteriorcingulate	−0.4329	0.0032[a]	−0.471	0.0006[a]		
Executive control network	Left caudal middle frontal	−0.397	0.0067[a]	−0.3728	0.0083[a]		
	Left parsorbitalis					−0.4969	0.0004[a]
	Left parstriangularis	−0.3408	0.0204	−0.4136	0.0051[a]		
	Left superiorparietal					−0.3755	0.0097[a]
	Left rostral middle frontal			−0.3961	0.0051[a]		
	Left superior frontal	−0.2982	0.0395	−0.3671	0.0102[a]		
	Left supramarginal	−0.335	0.0232			−0.3782	0.0072
	Right parsorbitalis	−0.3446	0.0176	−0.347	0.0188[a]	−0.4042	0.0041[a]
	Right rostralmiddlefrontal	−0.5574	0.0001[a]	−0.5669	0.00001[a]	−0.4544	0.001[a]
	Right superiorfrontal	−0.3354	0.0224	−0.3765	0.0088[a]	−0.4441	0.002[a]
	Right supramarginal					−0.3117	0.0327
Temporal lobe	Left banks of temporal lobe	−0.3856	0.0074	−0.4382	0.0020[a]	−0.3938	0.007[a]
	Left inferior temporal			−0.3887	0.0067[a]		
	Left middle temporal	−0.4234	0.0029[a]	−0.4267	0.0026[a]	−0.3373	0.0190
	Left superior temporal					−0.3616	0.0126[a]
	Left temporal pole			−0.3910	0.0060[a]	−0.5105	0.0002
	Right inferior temporal			−0.4088	0.0044[a]	−0.4598	0.0013[a]
	Right lingual					−0.4439	0.0016[a]
	Left lingual			−0.3779	0.0076[a]		
	Right superior temporal					−0.3129	0.0329
	Right temporal pole	−0.4283	0.0031[a]	−0.6476	0.00002[a]	−0.4516	0.0011[a]
Frontal	Left lateral orbitofrontal					−0.3426	0.0173
	Left medial orbitofrontal	−0.3097	0.0374	−0.4874	0.0009[a]	−0.2892	0.0494
	Right lateral orbitofrontal			−0.421	0.0028[a]		
	Right medial orbitofrontal			−0.422	0.0026[a]	−0.4624	0.0009[a]
	Right frontalpole	−0.3941	0.0069[a]	−0.4443	0.0022[a]	−0.3861	0.0066[a]
Other	Brain Stem	−0.3005	0.041[a]	−0.3032	0.0388		
	Left postcentral	−0.4782	0.0011[a]	−0.4801	0.0003[a]		
	Right lateral occipital	−0.434	0.0024[a]	−0.3399	0.0211	−0.5198	0.0002[a]
	Right paracentral			−0.3225	0.0265	−0.3437	0.0182

[a] Indicates region survived critical FDR threshold for multiple comparisons.

amygdala, caudate, and putamen, regions often neglected in cognitive neuroscience research.

Highly creative females demonstrated inverse relationships across all three measures examined. Global connectivity is the general connectedness of a network, the sum of the weights of all of the connections in the network. For highly creative females, fewer and/or less strong connections were observed, indicated by a lower overall connectivity measure. When the specific nodes of the networks were examined, we observed the same inverse relationships, varying in magnitude across the regions of the brain. This inverse relationship is consistent with previous reports finding lower levels of FA within the left anterior thalamic radiation (Jung et al., 2010a), here suggesting decreased connectivity across multiple regions of the brain.

The inverse relationships between global clustering and node specific measures of efficiency and clustering suggest that highly creative women have less local connectivity across the brain (van den Heuvel and Sporns, 2011; van den Heuvel et al., 2009). It is well established that the small-world organization of the structural connections of the brain facilitate efficient information transfer in the brain (Bassett and Bullmore, 2006). Interestingly, based on the inverse correlations found in females, these results suggest that more creative females have less segregated processing, with their brain networks perhaps resembling more simplistic random networks in terms of the lower clustering observed. Small world networks maximize efficiency with minimum cost (number of paths) (Bassett and Bullmore, 2006). While speculative, less clustering in creative females might imply reliance on more

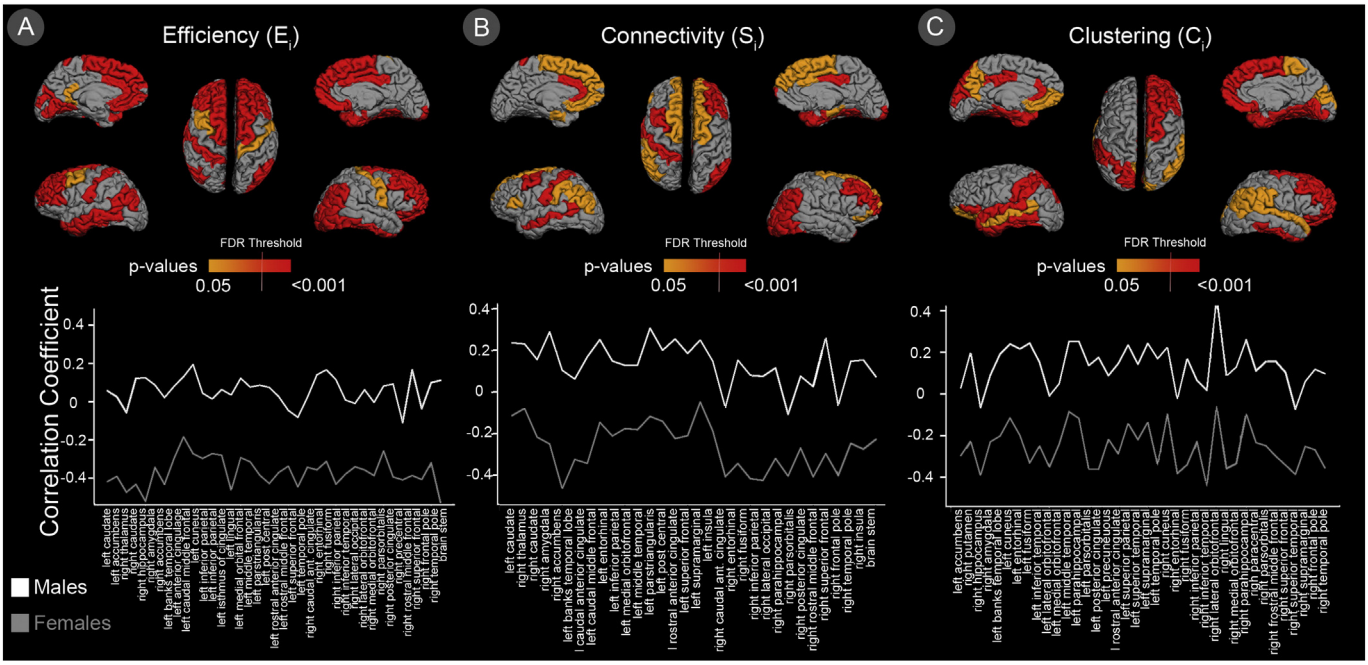

Fig. 3. Regions that significantly differ in correlations between graph metrics and creativity in males and females. Upper figures show p-values of significant differences in correlations, color bar indicates magnitude of p-value. Red line indicates critical FDR threshold ($q = 0.05$; see Materials and methods). Lower figures show correlations between creativity and graph metric for each of the significantly different individual regions with females shown in grey and males shown in white. A, Efficiency E_i is the average inverse shortest path length from each region to all other regions. B, Connectivity S_i is the sum of the connections of each region to all other regions. C, clustering C_i is the number of connections between all neighbor nodes of the region.

distributed processing, again suggesting involvement of more widespread regions. In contrast, highly creative males demonstrate more direct paths (connections between nodes have to pass through fewer nodes to reach destination) and greater clustering (more nearby neighbors of a node are connected). This organization is known to facilitate efficient information processing (Bassett and Bullmore, 2006), perhaps indicating that highly creative males rely on more locally oriented processing.

We found that many of the regions that demonstrate particularly strong relationships between efficiency, clustering and creativity were within the DMN and the ECN; however, the results were not limited to these networks. These networks are implicated in cognitive abilities required for the development of novel and useful ideas, but they also contribute to a vast array of other cognitive domains (i.e., attention, working memory, visualization, self-reflection), all of which interact with the ability to think divergently. Studies of divergent thinking have examined the extent to which the DMN becomes deactivated in cognitive tasks. Takeuchi et al. (2011) found that decreased task-induced deactivation (TID) of the precuneus of the DMN during a working memory task correlated to higher measures of divergent thinking. The magnitude of TID of the DMN has been hypothesized to reflect the reallocation of attention from task irrelevant to task relevant cognition (Mckiernan et al., 2003). Highly creative individuals demonstrate increased DMN activation during cognitive tasks (Takeuchi et al., 2012). Furthermore, divergent thinking is positively related to the connectivity between the MPFC and the PCC, suggesting increased fidelity of the DMN in highly creative individuals (Takeuchi et al., 2012).

While these studies support the notion of increased involvement of the DMN in creative cognition, they fail to address the involvement of the executive control network (ECN), regions of the frontal and parietal lobe that are also implicated in creativity (Ellamil et al., 2012; Liu et al., 2012), primarily the dorsolateral prefrontal cortex (DLPFC), the ventral prefrontal cortex (vPFC), and the lateral parietal cortex (Seeley et al., 2007). One study utilized a paradigm in which the individual was asked to first generate ideas in the scanner and separately evaluate and select the best ideas (Ellamil et al., 2012). These authors found that both the ECN and DMN were active during the evaluations of the ideas, whereas the temporal lobe was important to the generation of ideas. Another fMRI study examined neural functioning during freestyle rap improvisation as a means to assess creative generation (Liu et al., 2012). Participants exhibited dissociated activity in the MPFC and DLPFC, with increased activation of the MPFC and decreased activation of the DLPFC during freestyle rap improvisation. One interpretation of this activation pattern would include the supervisory attention and executive control mechanisms of the DLPFC being down-regulated, allowing for the generation of novel ideas.

A more comprehensive understanding of the how these specific cognitive abilities contribute to creative cognition will be necessary to begin to understand how variation in the underlying structure of these networks constrains the manifestation of creative ability. As the functional networks are constrained by the large-scale anatomical network structure (Greicius et al., 2009; Honey et al., 2009; van den Heuvel and Sporns, 2013a,b; van den Heuvel et al., 2009), the results of this study are expected to be reflected in the functional architectures. However, to our knowledge, there are no studies that have yet examined how creative cognition relates to the functional network architecture using measures of efficiency and clustering.

We have focused on the relationships between graph metrics and creativity in females, intentionally avoiding discussion of the relationships observed in males, as there were only weak effects that did not generally survive correction for multiple comparisons. A more important question is why females might exhibit strong relationships between network organization and creativity as opposed to males. The studies of sex differences in structural organization highlight the nature of the cognitive strengths of males and females (Gong et al., 2009a; Ingalhalikar et al., 2013). Specifically, Gong et al. (2009a,b) discussed female's advantage in aspects of verbal processing as a potential reason for the increased efficiency found within the left hemisphere.

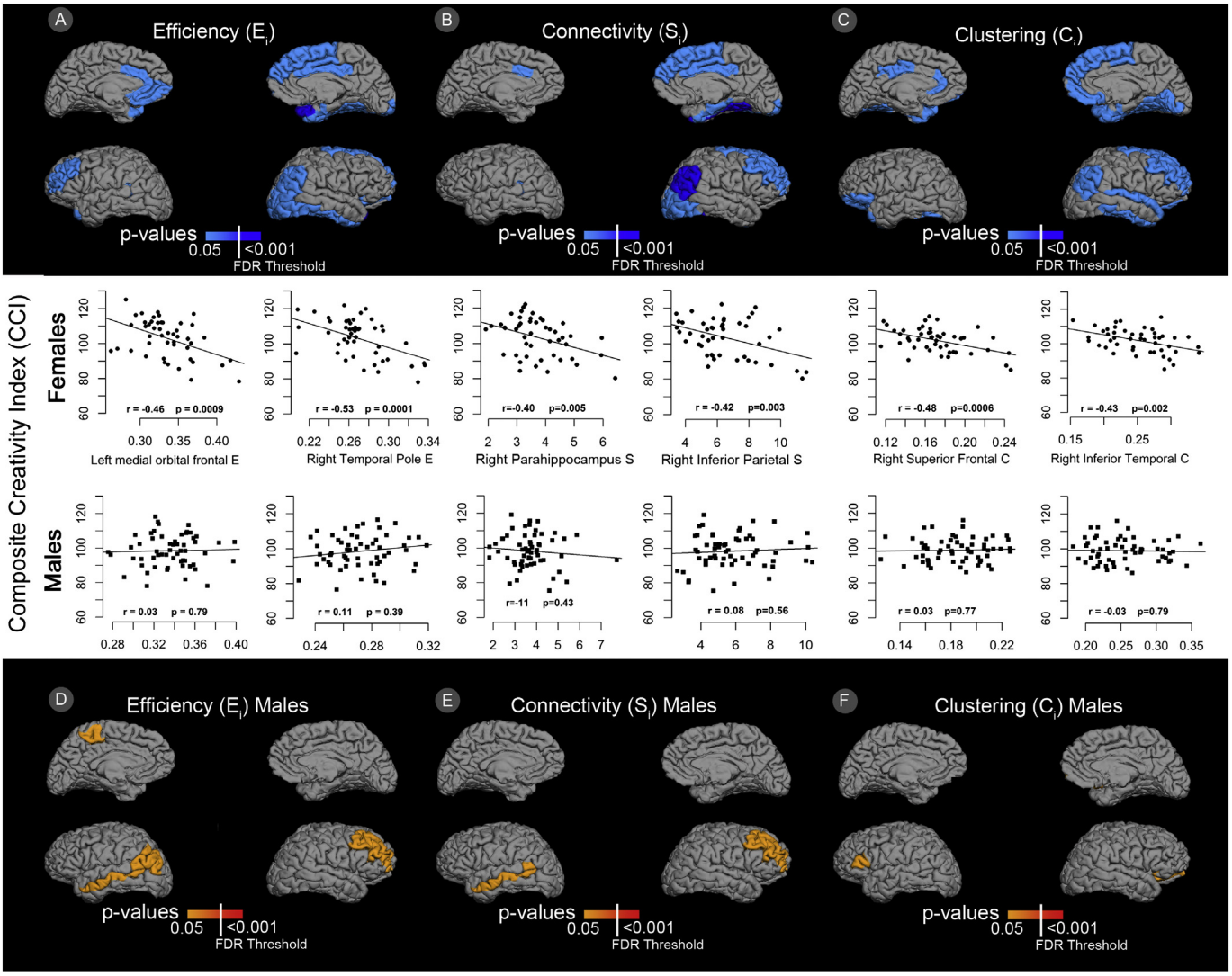

Fig. 4. Regions that have significant relationships between graph metric and creativity. Figures show p-values of significant differences in correlations, color bar indicates magnitude of p-value. Upper figures show significant relationships in females where the blue indicates that the relationship was inverse, where decreased measure of graph metric was related to increased creativity. Lower figures show significant relationships in males where orange to red indicates that the relationship was positive, increased graph metric was related to increased creativity. Line through color bar indicates critical FDR threshold ($q = 0.05$; see Materials and methods).

Ingalhalikar et al. (2013), in contrast, found that female brains exhibit increased inter hemispheric connectivity, whereas, males had more intra hemispheric connections. These authors suggest that females are better able to integrate information across the hemispheres, whereas males are better able to conduct coordinated action.

There are several limitations to consider when interpreting the results of this study. It is possible that we did not find substantial relationships between network architecture and creativity in males because we did not examine the network measures that are relevant in this group, such as modularity and transitivity as examined by Ingalhalikar et al. (2013). Other potential weaknesses of the study include the relatively small sample size (~100), the focus on measures of divergent thinking as a proxy for creative cognition, and the lack of functional graph measures (e.g., fMRI) by which to compare structural networks. The diffusion tensor model used to construct the fiber tracts may not accurately characterize tracts at points of complex fiber architecture (for example when tracts cross or kiss). Furthermore, this study only used one relatively low parcellation scheme and did not examine alternate edge weights beyond FA weighted and number of streamline weighted networks. Future studies should use higher quality diffusion data allowing for more advanced models of diffusion reconstruction that can resolve crossing fibers, multiple parcellation schemes, as well as different edge weights. Lastly, it is unclear how these metrics relate to global measures of grey and white matter volumes. Future studies should identify how global differences in gray matter and white matter affect the relationships between graph metrics and cognitive abilities.

This study provides initial data relevant to our understanding of sex differences in the relationships between structural networks and creativity. Emerging applications of complex network theory to the analysis of brain connectivity will provide a more sophisticated means of identifying the nature of the differences in network structure underlying individual differences in creative cognition. Moreover, such applications of graph theory should increase substantially our understanding of the interplay between complex cognitive constructs (e.g., creativity) with discrete functional brain networks.

Acknowledgments

This work was supported by the John Templeton Foundation — # 22156: "The Neuroscience of Scientific Creativity." The research of MPvdH was supported by a VENI grant (451-12-001) of the Dutch Research Council (NWO).

References

Achard, S., Salvador, R., Whitcher, B., Suckling, J., Bullmore, E., 2006. A resilient, low-frequency, small-world human brain functional network with highly connected association cortical hubs. J. Neurosci. 26, 63–72.

Amabile, T.M., 1982. Social psychology of creativity: a consensual assessment technique. J. Pers. Soc. Psychol. 43, 997–1013.

Arden, R., Chavez, R.S., Grazioplene, R., Jung, R.E., 2010. Neuroimaging creativity: a psychometric view. Behav. Brain Res. 214, 143–156.

Bassett, D.S., Bullmore, E., 2006. Small-world brain networks. Neuroscientist 12, 512–523.

Benjamini, Y., Hochberg, Y., 1995. Controlling the false discovery rate: a practical and powerful approach to multiple testing. J. R. Stat. Soc. Ser. B Methodol. 289–300.

Buckner, R.L., Carroll, D.C., 2007. Self-projection and the brain. Trends Cogn. Sci. 11, 49–57.

Buckner, R.L., Andrews-Hanna, J.R., Schacter, D.L., 2008. The brain's default network. Ann. N. Y. Acad. Sci. 1124, 1–38.

Bullmore, E., Sporns, O., 2009. Complex brain networks: graph theoretical analysis of structural and functional systems. Nat. Rev. Neurosci. 10, 186–198.

Campbell, D.T., 1960. Blind variation and selective retentions in creative thought as in other knowledge processes. Psychol. Rev. 67, 380.

Chang, L.C., Jones, D.K., Pierpaoli, C., 2005. RESTORE: robust estimation of tensors by outlier rejection. Magn. Reson. Med. 53, 1088–1095.

Craddock, R.C., Jbabdi, S., Yan, C.-G., Vogelstein, J.T., Castellanos, F.X., Di Martino, A., Kelly, C., Heberlein, K., Colcombe, S., Milham, M.P., 2013. Imaging human connectomes at the macroscale. Nat. Methods 10, 524–539.

de Haan, W., van der Flier, W.M., Koene, T., Smits, L., Scheltens, P., Stam, C.J., 2012. Disrupted modular brain dynamics reflect cognitive dysfunction in Alzheimer's disease. Neuroimage 59, 3085–3093.

Eguiluz, V.M., Chialvo, D.R., Cecchi, G.A., Baliki, M., Apkarian, A.V., 2005. Scale-free brain functional networks. Phys. Rev. Lett. 94, 18102.

Ellamil, M., Dobson, C., Beeman, M., Christoff, K., 2012. Evaluative and generative modes of thought during the creative process. Neuroimage 59, 1783–1794.

Fair, D.A., Posner, J., Nagel, B.J., Bathula, D., Dias, T.G.C., Mills, K.L., Blythe, M.S., Giwa, A., Schmitt, C.F., Nigg, J.T., 2010. Atypical default network connectivity in youth with attention-deficit/hyperactivity disorder. Biol. Psychiatry 68, 1084–1091.

Fischl, B., Van Der Kouwe, A., Destrieux, C., Halgren, E., Ségonne, F., Salat, D.H., Busa, E., Seidman, L.J., Goldstein, J., Kennedy, D., 2004. Automatically parcellating the human cerebral cortex. Cereb. Cortex 14, 11–22.

Gansler, D.A., Moore, D.W., Susmaras, T.M., Jerram, M.W., Sousa, J., Heilman, K.M., 2011. Cortical morphology of visual creativity. Neuropsychologia 49, 2527–2532.

Gong, G., Rosa-Neto, P., Carbonell, F., Chen, Z.J., He, Y., Evans, A.C., 2009a. Age-and gender-related differences in the cortical anatomical network. J. Neurosci. 29, 15684–15693.

Gong, G.L., Rosa, P., Carbonell, F., Chen, Z.J., He, Y., Evans, A.C., 2009b. Age- and gender-related differences in the cortical anatomical network. J. Neurosci. 29, 15684–15693.

Gong, G., He, Y., Evans, A.C., 2011. Brain connectivity: gender makes a difference. Neuroscientist 17, 575–591.

Greicius, M.D., Krasnow, B., Reiss, A.L., Menon, V., 2003. Functional connectivity in the resting brain: a network analysis of the default mode hypothesis. Proc. Natl. Acad. Sci. 100, 253–258.

Greicius, M.D., Supekar, K., Menon, V., Dougherty, R.F., 2009. Resting-state functional connectivity reflects structural connectivity in the default mode network. Cereb. Cortex 19, 72–78.

Gur, R.C., Turetsky, B.I., Matsui, M., Yan, M., Bilker, W., Hughett, P., Gur, R.E., 1999. Sex differences in brain gray and white matter in healthy young adults: correlations with cognitive performance. J. Neurosci. 19, 4065–4072.

Hagmann, P., Cammoun, L., Gigandet, X., Meuli, R., Honey, C.J., Wedeen, V.J., Sporns, O., 2008. Mapping the structural core of human cerebral cortex. PLoS Biol. 6, e159.

Haier, R.J., Jung, R.E., Yeo, R.A., Head, K., Alkire, M.T., 2005. The neuroanatomy of general intelligence: sex matters. Neuroimage 25, 320–327.

Honey, C., Sporns, O., Cammoun, L., Gigandet, X., Thiran, J.-P., Meuli, R., Hagmann, P., 2009. Predicting human resting-state functional connectivity from structural connectivity. Proc. Natl. Acad. Sci. 106, 2035–2040.

Humphries, M.D., Gurney, K., 2008. Network 'small-world-ness': a quantitative method for determining canonical network equivalence. PLoS One 3, e0002051.

Ingalhalikar, M., Smith, A., Parker, D., Satterthwaite, T.D., Elliott, M.A., Ruparel, K., Hakonarson, H., Gur, R.E., Gur, R.C., Verma, R., 2013. Sex differences in the structural connectome of the human brain. Proc. Natl. Acad. Sci. http://dx.doi.org/10.1073/pnas.1316909110.

Johansen-Berg, H., Behrens, T.E., 2009. Diffusion MRI: From Quantitative Measurement to In-vivo Neuroanatomy (Access Online via Elsevier).

Jung, R.E., Haier, R.J., Yeo, R.A., Rowland, L.M., Petropoulos, H., Levine, A.S., Sibbitt, W.L., Brooks, W.M., 2005. Sex differences in N-acetylaspartate correlates of general intelligence: an ^{1}H-MRS study of normal human brain. Neuroimage 26, 965–972.

Jung, R.E., Grazioplene, R., Caprihan, A., Chavez, R.S., Haier, R.J., 2010a. White matter integrity, creativity, and psychopathology: disentangling constructs with diffusion tensor imaging. PLoS One 5, e9818.

Jung, R.E., Segall, J.M., Jeremy Bockholt, H., Flores, R.A., Smith, S.M., Chavez, R.S., Haier, R.J., 2010b. Neuroanatomy of creativity. Hum. Brain Mapp. 31, 398–409.

Jung, R., Mead, B., Carrasco, J., Flores, R., 2013. The structure of creative cognition in the human brain. Front. Hum. Neurosci. 7, 330.

Latora, V., Marchiori, M., 2001. Efficient behavior of small-world networks. Phys. Rev. Lett. 87, 198701.

Lezak, M.D., Howieson, D.B., Loring, D.W., 2004. Neuropsychological Assessment. Oxford University Press, USA.

Li, Y., Liu, Y., Li, J., Qin, W., Li, K., Yu, C., Jiang, T., 2009. Brain anatomical network and intelligence. PLoS Comput. Biol. 5, e1000395.

Liu, S., Chow, H.M., Xu, Y., Erkkinen, M.G., Swett, K.E., Eagle, M.W., Rizik-Baer, D.A., Braun, A.R., 2012. Neural correlates of lyrical improvisation: an fMRI study of freestyle rap. Scientific Reports, 2.

Mckiernan, K.A., Kaufman, J.N., Kucera-Thompson, J., Binder, J.R., 2003. A parametric manipulation of factors affecting task-induced deactivation in functional neuroimaging. J. Cogn. Neurosci. 15, 394–408.

Miller, G.F., Tal, I.R., 2007. Schizotypy versus openness and intelligence as predictors of creativity. Schizophr. Res. 93, 317–324.

Mori, S., van Zijl, P.C., 2002. Fiber tracking: principles and strategies — a technical review. NMR Biomed. 15, 468–480.

Piffer, D., 2012. Can creativity be measured? An attempt to clarify the notion of creativity and general directions for future research. Think. Skills Creat. 7, 258–264.

Raichle, M.E., MacLeod, A.M., Snyder, A.Z., Powers, W.J., Gusnard, D.A., Shulman, G.L., 2001. A default mode of brain function. Proc. Natl. Acad. Sci. 98, 676–682.

Rubinov, M., Sporns, O., 2010. Complex network measures of brain connectivity: uses and interpretations. Neuroimage 52, 1059–1069.

Schmithorst, V.J., 2009. Developmental sex differences in the relation of neuroanatomical connectivity to intelligence. Intelligence 37, 164–173.

Schmithorst, V.J., Holland, S.K., 2007. Sex differences in the development of neuroanatomical functional connectivity underlying intelligence found using Bayesian connectivity analysis. Neuroimage 35, 406–419.

Seeley, W.W., Menon, V., Schatzberg, A.F., Keller, J., Glover, G.H., Kenna, H., Reiss, A.L., Greicius, M.D., 2007. Dissociable intrinsic connectivity networks for salience processing and executive control. J. Neurosci. 27, 2349–2356.

Shulman, G.L., Fiez, J.A., Corbetta, M., Buckner, R.L., Miezin, F.M., Raichle, M.E., Petersen, S.E., 1997. Common blood flow changes across visual tasks: II. Decreases in cerebral cortex. J. Cogn. Neurosci. 9, 648–663.

Smith, S.M., Jenkinson, M., Johansen-Berg, H., Rueckert, D., Nichols, T.E., Mackay, C.E., Watkins, K.E., Ciccarelli, O., Cader, M.Z., Matthews, P.M., 2006. Tract-based spatial statistics: voxelwise analysis of multi-subject diffusion data. Neuroimage 31, 1487–1505.

Sporns, O., Chialvo, D.R., Kaiser, M., Hilgetag, C.C., 2004. Organization, development and function of complex brain networks. Trends Cogn. Sci. 8, 418–425.

Stam, C.J., Reijneveld, J.C., 2007a. Graph theoretical analysis of complex networks in the brain. Nonlinear Biomed. Phys. 1, 3.

Stam, C.J., Reijneveld, J.C., 2007b. Graph theoretical analysis of complex networks in the brain. Nonlinear Biomed. Phys. 1.

Stein, M.I., 1953. Creativity and culture. J. Psychol. 36, 311–322.

Takeuchi, H., Taki, Y., Sassa, Y., Hashizume, H., Sekiguchi, A., Fukushima, A., Kawashima, R., 2010a. Regional gray matter volume of dopaminergic system associate with creativity: evidence from voxel-based morphometry. Neuroimage 51, 578–585.

Takeuchi, H., Taki, Y., Sassa, Y., Hashizume, H., Sekiguchi, A., Fukushima, A., Kawashima, R., 2010b. White matter structures associated with creativity: evidence from diffusion tensor imaging. Neuroimage 51, 11–18.

Takeuchi, H., Taki, Y., Hashizume, H., Sassa, Y., Nagase, T., Nouchi, R., Kawashima, R., 2011. Failing to deactivate: the association between brain activity during a working memory task and creativity. Neuroimage 55, 681–687.

Takeuchi, H., Taki, Y., Hashizume, H., Sassa, Y., Nagase, T., Nouchi, R., Kawashima, R., 2012. The association between resting functional connectivity and creativity. Cereb. Cortex 22 (12), 2921–2929.

van den Heuvel, M.P., Sporns, O., 2011. Rich-club organization of the human connectome. J. Neurosci. 31, 15775–15786.

van den Heuvel, M.P., Sporns, O., 2013a. An anatomical substrate for integration among functional networks in human cortex. J. Neurosci. 33, 14489–14500.

van den Heuvel, M.P., Sporns, O., 2013b. Network hubs in the human brain. Trends Cogn. Sci. 17, 683–696.

van den Heuvel, M.P., Stam, C.J., Boersma, M., Hulshoff Pol, H.E., 2008. Small-world and scale-free organization of voxel-based resting-state functional connectivity in the human brain. NeuroImage 43, 528–539.

van den Heuvel, M.P., Stam, C.J., Kahn, R.S., Pol, H.E.H., 2009. Efficiency of functional brain networks and intellectual performance. J. Neurosci. 29, 7619–7624.

van den Heuvel, M.P., Mandl, R.C., Stam, C.J., Kahn, R.S., Pol, H.E.H., 2010. Aberrant frontal and temporal complex network structure in schizophrenia: a graph theoretical analysis. J. Neurosci. 30, 15915–15926.

Watts, D., Strogatz, S., 1998a. The small world problem. Collec. Dyn. Small-World Netw. 393, 440–442.

Watts, D.J., Strogatz, S.H., 1998b. Collective dynamics of 'small-world' networks. Nature 393, 440–442.

Wechsler, D., 1981. The psychometric tradition: developing the Wechsler adult intelligence scale. Contemp. Educ. Psychol. 6 (2), 82–85.